Limiting Kinetic Energy through Control Barrier Functions: Analysis and Experimental Validation

Daniël Logmans

***Abstract*—An energy-based Control Barrier Function (CBF) is used to limit kinetic energy of torque-controlled robots. The proposed CBF produces a safety-critical control action that bounds the kinetic energy of the manipulator by purely injecting damping in the underlying closed-loop system, not compromising its passivity and stability properties. We present an extensive experimental validation of the approach on a 7-Degree of Freedom (DoF) Franka Emika Panda robot.**

I. Introduction

OPERATOR safety is the most critical control objective when humans and robots start sharing the same space. The recent rise of learning based controllers, which often only provide probabilistic safety guarantees, has underscored the need for safety-critical approaches to robot operation [1].

This need has led to various ISO standards and is addressed in many published works [2]. Some prevent interaction by enforcing a speed-dependent separation distance between the robot and operator, assuming reliable detection methods [3], where other works limit long-duration interaction power and force by implementing e.g. impedance control [4], [5]. Haddadin et al. explore various dynamic human-robot impact scenarios and relate the impact velocity to the risk of injury [6].

In this work, safety is addressed by constraining the kinetic energy that could potentially be transferred to a human operator, to prevent injury in collision scenarios. This takes the form of a *safety filter* that enforces this constraint while minimally altering the desired control input. We make use of Control Barrier Functions (CBFs), which constrain the robot to a 'safe' subset of the state space [7]. Many CBF implementations only demonstrate kinematic control and rely on lower-level controllers to handle system dynamics [8], [9], [10]. Instead, we investigate the use of energy-based CBFs and, different from previous works like [11] and [12], utilize them to limit the kinetic energy of a torque-controlled robot.

Recent work by Michel et al. presents a control scheme that also limits the kinetic energy. This is achieved by augmenting the dynamics of an energy tank and integrating higher-order CBF schemes. Passivity is enforced by the energy tank architecture [13]. Our work presents a different approach, for which we show that our proposed safety-critical CBF only injects damping into the system. As a result, the safety-critical control action structurally preserves the passivity of the nominal closed-loop system without the need for additional frameworks. We experimentally validate the performance of our proposed safety filter on a 7-DoF robotic manipulator.

The main contributions of this paper are as follows:

1) A kinetic energy-limiting CBF-based safety filter and analysis of its energetic properties and disturbance rejection.
2) Extensive experimental validation of the proposed safety-critical control system.

To the best of the author's knowledge, this is the first time that this form of control is validated experimentally on a robotic manipulator.

The remainder of this paper is outlined as follows. Sec. II of this work describes the mathematical background of this control approach. We validate the control system for three different scenarios in Sec. III.

II. Methods

In this section, we present a brief mathematical description of the CBF control approach. The general form of CBFs is described first, after which we present our energy-based approach.

A. Control Barrier Function background

Control Barrier Functions allow us to keep a system within a given safe set while minimally altering the desired control input. This section introduces the general concept of CBFs [7]. Given a nonlinear control-affine system

$$\dot{\boldsymbol{x}} = f(\boldsymbol{x}) + g(\boldsymbol{x})\boldsymbol{u} \tag{1}$$

with system state $\boldsymbol{x} \in \mathcal{D} \subset \mathbb{R}^n$ and control input $\boldsymbol{u} \in \mathcal{U} \subset \mathbb{R}^m$. $f(\boldsymbol{x})$ and $g(\boldsymbol{x})$ are assumed to be locally Lipschitz. We define a safe set $\mathcal{S} \subset \mathcal{D}$ which contains all allowed (safe) states. More specifically, it is defined as the superlevel set of a continuously differentiable function $h(\boldsymbol{x}) : \mathcal{D} \to \mathbb{R}$, i.e. all states for which $h(\boldsymbol{x})$ is positive:

$$\mathcal{S} = \{\boldsymbol{x} \in \mathcal{D} \subset \mathbb{R}^n : h(\boldsymbol{x}) \geq 0\}. \tag{2}$$

The relative degree of h is the number of times that h needs to be differentiated with respect to time before the input $\boldsymbol{u}$ appears explicitly in the expression.

h is a CBF if it has a relative degree of 1 and there exists a $\boldsymbol{u}$ in the set of feasible control inputs $\mathcal{U}$ such that for all $\boldsymbol{x} \in \mathcal{S}$,

$$\sup_{\boldsymbol{u} \in \mathcal{U}} \underbrace{\left[\frac{\partial h}{\partial \boldsymbol{x}} f(\boldsymbol{x}) + \frac{\partial h}{\partial \boldsymbol{x}} g(\boldsymbol{x})\boldsymbol{u}\right]}_{\dot{h}(\boldsymbol{x},\boldsymbol{u})} \geq -\alpha(h(\boldsymbol{x})). \tag{3}$$

Here, α is an extended class $\mathcal{K}_\infty$ function.[1] For our purposes, $\alpha(h) \equiv \gamma h$, with γ a positive real number, suffices.

Theorem 1 (Ames et al. [7])**.** *Let Eq.* (3) *be true for the control affine system (1). If the system starts in $\mathcal{S}$, it will never leave it. $\mathcal{S}$ is therefore forward-invariant:*

$$\boldsymbol{x}(0) \in \mathcal{S} \rightarrow \boldsymbol{x}(t) \in \mathcal{S} \text{ for all } t \geq 0. \tag{4}$$

Moreover, if Eq. (3) *holds for all $\boldsymbol{x} \in \mathcal{D}$, the requirement not only makes $\mathcal{S}$ invariant, but also asymptotically stable: a system outside the safe set will be driven towards it.*

CBFs are typically implemented as a safety filter to modify the input of a primary ('nominal') controller $\boldsymbol{u}_{\text{des}}$ as little as possible to make it satisfy the safety condition:

$$\begin{aligned} &\boldsymbol{u} = \text{argmin}_{\boldsymbol{u}^*} ||\boldsymbol{u}^* - \boldsymbol{u}_{\text{des}}||^2 \\ &\text{subject to } \Psi(\boldsymbol{x}, \boldsymbol{u}) \geq 0, \end{aligned} \tag{5}$$

where

$$\Psi(\boldsymbol{x}, \boldsymbol{u}) = \dot{h}(\boldsymbol{x}, \boldsymbol{u}) + \alpha(h(\boldsymbol{x})). \tag{6}$$

Note that multiple CBFs may have to be satisfied congruently instead of just the one shown here. This optimization problem can be rewritten to a standard-form Quadratic Program (QP) and solved numerically, or, in the case of a single CBF, an analytic solution can be derived.

B. Main contribution: Kinetic energy as safe set

We present a type of CBF that has the primary objective of limiting kinetic energy. We consider a system configuration vector $\boldsymbol{q}$ and the system's Euler-Lagrange dynamic equation:[2]

$$\boldsymbol{D}(\boldsymbol{q})\ddot{\boldsymbol{q}} + \boldsymbol{C}(\boldsymbol{q}, \dot{\boldsymbol{q}})\dot{\boldsymbol{q}} + \boldsymbol{G}(\boldsymbol{q}) = \boldsymbol{B}\boldsymbol{u}, \tag{7}$$

with $\boldsymbol{D}(\boldsymbol{q})$ the inertial matrix, $\boldsymbol{C}(\boldsymbol{q}, \dot{\boldsymbol{q}})$ the Coriolis matrix, $\boldsymbol{G}(\boldsymbol{q})$ the gravity vector and $\boldsymbol{B}$ the actuation matrix. Note that friction is neglected here. The energy-based CBF proposed in this work is given by the kinetic energy limit $K_{\max}$ minus the kinetic energy K:

$$h(\boldsymbol{q}, \dot{\boldsymbol{q}}) = K_{\max} - K(\boldsymbol{q}, \dot{\boldsymbol{q}}) = K_{\max} - \frac{1}{2}\dot{\boldsymbol{q}}^\top \boldsymbol{D}(\boldsymbol{q})\dot{\boldsymbol{q}}. \tag{8}$$

This yields the safety constraint $\dot{K} \leq \alpha(K_{\max} - K)$, or, given a fully actuated system:

$$\underbrace{-\dot{\boldsymbol{q}}^\top \boldsymbol{B}\boldsymbol{u} + \dot{\boldsymbol{q}}^\top \boldsymbol{G}(\boldsymbol{q})}_{\dot{h}(\boldsymbol{q}, \dot{\boldsymbol{q}}, \boldsymbol{u})} \geq -\alpha\left(K_{\max} - \frac{1}{2}\dot{\boldsymbol{q}}^\top \boldsymbol{D}(\boldsymbol{q})\dot{\boldsymbol{q}}\right). \tag{9}$$

The two power terms on the left imply that the CBF safety layer will only intervene when the mechanical power input to the system would be too high, dissipating energy to keep it within safe limits.

[1] A strictly increasing continuous function $\alpha : \mathbb{R} \rightarrow \mathbb{R}$ with $\alpha(0) = 0$.

[2] Note that this expression can easily be rewritten as an affine control system (Eq. (1)) if $\boldsymbol{x}$ contains $\boldsymbol{q}$ and $\dot{\boldsymbol{q}}$.

Theorem 2. *Let (8) be the CBF acting on control system (7) where the control input is given by Eq.* (5) *and let $\boldsymbol{u}_{\text{safe}} = (\boldsymbol{u} - \boldsymbol{u}_{\text{des}})$ be the safety filter control input. Then the total power injected by the safety filter is always negative, that is,*

$$P_{\text{safe}} = \dot{\boldsymbol{q}}^\top \boldsymbol{B}\boldsymbol{u}_{\text{safe}} \leq 0. \tag{10}$$

Proof. If $\Psi(\boldsymbol{q}, \dot{\boldsymbol{q}}, \boldsymbol{u}_{\text{des}}) \geq 0$, the safety constraint of Eq. (5) is already satisfied and $\boldsymbol{u} = \boldsymbol{u}_{\text{des}}$. The power input by the safety later is then 0. Therefore, we only consider $\Psi(\boldsymbol{q}, \dot{\boldsymbol{q}}, \boldsymbol{u}_{\text{des}}) < 0$.

Eq. (10) is equivalent to

$$\dot{\boldsymbol{q}}^\top \boldsymbol{B}\boldsymbol{u} \leq \dot{\boldsymbol{q}}^\top \boldsymbol{B}\boldsymbol{u}_{\text{des}}. \tag{11}$$

The CBF enforces the following safety constraint on the control power (Eq. (9)):

$$\dot{\boldsymbol{q}}^\top \boldsymbol{B}\boldsymbol{u} \leq \alpha(h(\boldsymbol{q}, \dot{\boldsymbol{q}})) + \dot{\boldsymbol{q}}^\top \boldsymbol{G}(\boldsymbol{q}). \tag{12}$$

If we can show that Eq. (12) always ensures Eq. (11), we prove the theorem. This means we have to prove the following relation:

$$\alpha(h(\boldsymbol{q}, \dot{\boldsymbol{q}})) + \dot{\boldsymbol{q}}^\top \boldsymbol{G}(\boldsymbol{q}) \leq \dot{\boldsymbol{q}}^\top \boldsymbol{B}\boldsymbol{u}_{\text{des}}, \tag{13}$$

which can be rewritten as

$$\dot{h}(\boldsymbol{q}, \dot{\boldsymbol{q}}, \boldsymbol{u}_{\text{des}}) + \alpha(h(\boldsymbol{q}, \dot{\boldsymbol{q}})) = \Psi(\boldsymbol{q}, \dot{\boldsymbol{q}}, \boldsymbol{u}_{\text{des}}) \leq 0. \tag{14}$$

This proves that the theorem also holds under the condition $\Psi(\boldsymbol{q}, \dot{\boldsymbol{q}}, \boldsymbol{u}_{\text{des}}) < 0$.

□

Califano shows in [14] that the damping property in Theorem 2 ensures preservation of passivity if the nominal controller is passive.

Theorem 3. *Let (8) be the CBF acting on a fully actuated control system (7) where the control input is given by Eq.* (5)*. Then the closed-form solution for the control input is given by:*

$$\boldsymbol{u} = \begin{cases} \frac{\boldsymbol{B}^\top \dot{\boldsymbol{q}}}{||\boldsymbol{B}^\top \dot{\boldsymbol{q}}||^2}\left(\dot{\boldsymbol{q}}^\top \boldsymbol{G}(\boldsymbol{q}) + \alpha(h(\boldsymbol{q}, \dot{\boldsymbol{q}}))\right) & \text{if } \Psi(\boldsymbol{q}, \dot{\boldsymbol{q}}, \boldsymbol{u}_{\text{des}}) < 0 \\ \boldsymbol{u}_{\text{des}} & \text{otherwise.} \end{cases} \tag{15}$$

Proof. We start from the analytical solution from [12], Eq. (15):

$$\boldsymbol{u} = \boldsymbol{u}_{\text{des}} + \begin{cases} \frac{\boldsymbol{B}^\top \dot{\boldsymbol{q}}}{||\boldsymbol{B}^\top \dot{\boldsymbol{q}}||^2}\Psi(\boldsymbol{q}, \dot{\boldsymbol{q}}, \boldsymbol{u}_{\text{des}}) & \text{if } \Psi(\boldsymbol{q}, \dot{\boldsymbol{q}}, \boldsymbol{u}_{\text{des}}) < 0 \\ 0 & \text{otherwise.} \end{cases} \tag{16}$$

For $\Psi(\boldsymbol{q}, \dot{\boldsymbol{q}}, \boldsymbol{u}_{\text{des}}) < 0$, substituting our CBF yields

$$\boldsymbol{u} = \boldsymbol{u}_{\text{des}} + \frac{\boldsymbol{B}^\top \dot{\boldsymbol{q}}}{||\boldsymbol{B}^\top \dot{\boldsymbol{q}}||^2}\left(-\dot{\boldsymbol{q}}^\top \boldsymbol{B}\boldsymbol{u}_{\text{des}} + \dot{\boldsymbol{q}}^\top \boldsymbol{G}(\boldsymbol{q}) + \alpha(h(\boldsymbol{q}, \dot{\boldsymbol{q}}))\right) \tag{17}$$

which simplifies to an expression that does not depend on $\boldsymbol{u}_{\text{des}}$:

$$\boldsymbol{u} = \frac{\boldsymbol{B}^\top \dot{\boldsymbol{q}}}{||\boldsymbol{B}^\top \dot{\boldsymbol{q}}||^2}\left(\dot{\boldsymbol{q}}^\top \boldsymbol{G}(\boldsymbol{q}) + \alpha(h(\boldsymbol{q}, \dot{\boldsymbol{q}}))\right). \tag{18}$$

□

Although not immediately obvious, the closed-form solution shown in Theorem 3 depends on the cube of the joint velocity when the CBF is 'active'.

Remark 1 (Relative degree problem)**.** *Sec. II-A mentions that the relative degree of the CBF has to be 1, implying that $\dot{h}$ should depend directly on $\boldsymbol{u}$. Many examples in literature demonstrate CBFs with, e.g., position-based obstacle avoidance and can only apply velocity inputs, since velocities are the first temporal derivative of position. The underlying torque controller is assumed to handle the dynamics and track the desired velocity input perfectly. The kinetic energy term in our CBF is velocity-dependent and can therefore be used for direct torque control. Singletary et al. use this property to extend higher-degree CBFs, solving the relative degree problem while still fulfilling the original CBF requirements [12]. For the CBF presented here, the kinetic energy safe set in and of itself is the primary objective. Like their work, our safety constraint is independent of the Coriolis matrix $\boldsymbol{C}(\boldsymbol{q}, \dot{\boldsymbol{q}})$, reducing model dependence and computational complexity.*

C. External interaction forces

The dynamic system presented in Eq. (7) does not include external torques caused by disturbances or interaction. For a known external torque $\boldsymbol{\tau}_{\text{ext}}$, one can extend Eq. (7):

$$\boldsymbol{D}(\boldsymbol{q})\ddot{\boldsymbol{q}} + \boldsymbol{C}(\boldsymbol{q}, \dot{\boldsymbol{q}})\dot{\boldsymbol{q}} + \boldsymbol{G}(\boldsymbol{q}) = \boldsymbol{B}\boldsymbol{u} + \boldsymbol{\tau}_{\text{ext}}. \tag{19}$$

If these torques are not taken into account, system invariance cannot be guaranteed.

Theorem 4. *Given an external positive power input $P_{\text{ext}} = \dot{\boldsymbol{q}}^\top \boldsymbol{\tau}_{\text{ext}}$, the maximum kinetic energy overshoot $K - K_{\max}$ is proportional to this power:*

$$K - K_{\max} \leq \frac{P_{\text{ext}}}{\gamma}. \tag{20}$$

Proof. The steady-state kinetic energy overshoot is reached when the total power flow into the system is zero. This power is delivered by the control input, gravity and the external torque. Using the analytic solution (Eq. (15)) to find the control power, we have the following power balance:

$$\underbrace{\dot{\boldsymbol{q}}^\top \boldsymbol{G}(\boldsymbol{q}) + \alpha(K_{\max} - K)}_{\dot{\boldsymbol{q}}^\top \boldsymbol{B}\boldsymbol{u}} - \dot{\boldsymbol{q}}^\top \boldsymbol{G}(\boldsymbol{q}) + P_{\text{ext}} = 0, \tag{21}$$

from which follows the error in kinetic energy:

$$K - K_{\max} = \alpha^{-1}(P_{\text{ext}}). \tag{22}$$

One can see that for $\alpha(h) = \gamma h$, we obtain Eq. (20). □

Theorem 4 leads to a conflicting requirement: increasing γ leads to a more conservative system, but also to poorer disturbance rejection. One can circumvent this by estimating the external interaction power and actively compensating for it. This leads to the following interaction-aware control requirement:

$$\underbrace{\dot{\boldsymbol{q}}^\top(-\boldsymbol{B}\boldsymbol{u} - \boldsymbol{\tau}_{\text{ext}} + \boldsymbol{G}(\boldsymbol{q}))}_{\dot{h}(\boldsymbol{q}, \dot{\boldsymbol{q}}, \boldsymbol{u})} \geq -\alpha\left(K_{\max} - \frac{1}{2}\dot{\boldsymbol{q}}^\top \boldsymbol{D}(\boldsymbol{q})\dot{\boldsymbol{q}}\right). \tag{23}$$

The challenge lies in predicting $\boldsymbol{\tau}_{\text{ext}}$, or, in practice, finding a good estimate $\hat{\boldsymbol{\tau}}_{\text{ext}}$. If accurately estimated, this control scheme will keep the kinetic energy below the desired limit. However, note that this may not always lead to a safer situation: the safety filter is designed to provide minimal damping, also when the external power is negative. We observe four cases:

1) Interaction-agnostic, $P_{\text{ext}} > 0$: $K \leq K_{\max} + \frac{P_{\text{ext}}}{\gamma}$.
2) Interaction-agnostic, $P_{\text{ext}} \leq 0$: $K \leq K_{\max}$.
3) Interaction-aware, $P_{\text{ext}} > 0$: P_{ext} fully dissipated, $K \leq K_{\max}$.
4) Interaction-aware, $P_{\text{ext}} \leq 0$: P_{ext} fully utilized for damping, $K \leq K_{\max}$.

So if an operator provides power, the interaction-aware controller will dissipate it. However, it will also leverage negative power provided by the external interaction (e.g. a human). This effectively means that the operator is exposed to the full power of the base controller if it stands in the way.

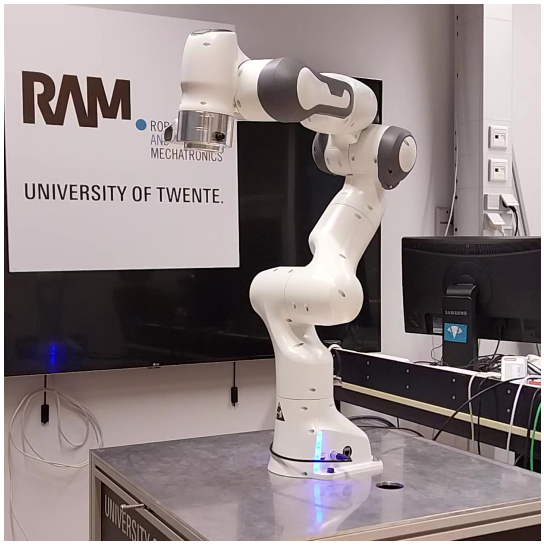

Fig. 1: The Franka Emika Panda robot used for the experiments.

III. Experimental results

A. Overview of experiments

We present three different experiments to validate the effectiveness of our approach:

1) A Cartesian step response.
2) A sudden loss of contact with the environment.
3) An external power input with and without external torque estimation and compensation.

The nominal control action for the first two experiments is an underdamped Cartesian impedance controller with a stiffness of 200 N/m and a damping ratio of 0.2. For the third experiment, the nominal controller is deactivated.[3]

For these experiments, we choose $\alpha(h) = \gamma h$. By decreasing γ, we expect increasingly conservative behavior.

B. Experimental Setup

The experimental validation is performed on the Franka Emika Panda 7-DoF fully actuated robotic arm displayed in

[3]Note that gravity compensation is still present.

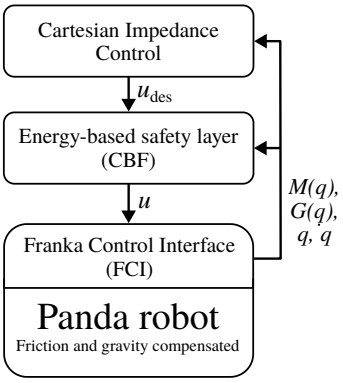

Fig. 2: Control architecture of the experimental setup.

Fig. 1. The Franka Control Interface (FCI) provides a ROS-interface for joint level torque commands at 1000 Hz, with built-in gravity and friction compensation. As a result, we set $\boldsymbol{G}(\boldsymbol{q}) \equiv \boldsymbol{0}$ in Eq. (7). At each interval, the interface provides the dynamics matrices $\boldsymbol{D}(\boldsymbol{q})$, $\boldsymbol{G}(\boldsymbol{q})$, $\boldsymbol{B}$, external torque estimation $\hat{\boldsymbol{\tau}}_{\text{ext}}$ and state information $\boldsymbol{q}$, $\dot{\boldsymbol{q}}$. A schematic representation of the controller configuration is provided in Fig. 2.

To reduce the effect of sensor noise on the velocity estimates, a discrete joint acceleration rate limiter is implemented:

$$\dot{\boldsymbol{q}}_k = \dot{\boldsymbol{q}}_{k-1} + \min(\max(\dot{\boldsymbol{q}}_k - \dot{\boldsymbol{q}}_{k-1}, -\Delta_t \ddot{\boldsymbol{q}}_{\max}), \Delta_t \ddot{\boldsymbol{q}}_{\max}) \quad (24)$$

where the maximum joint acceleration $\ddot{\boldsymbol{q}}_{\max}$ is set to the robot's documented limits plus a 20% margin. Δ_t is the time interval between consecutive measurements $\boldsymbol{q}_k$ and $\boldsymbol{q}_{k+1}$. The benefit of an acceleration saturation filter is that it does not introduce any lag and enforces an upper bound on the noise amplitude without attenuating the signal itself.

Despite the existence of an analytical solution (15) to the QP (5), our implementation leverages the OSQP quadratic program solver [15]. The reason is that the analytical solution does not allow including input saturation limits or stacking of additional (CBF) constraints. The solver operates on an Intel® Core™ i7-7700 processor and sufficient convergence to the analytical solution is reached well within the 1 ms control loop constraint.

C. Step response

In this experiment, the equilibrium setpoint is moved by 40 cm in the (horizontal) y-direction by a square wave signal. When the safety filter is active, the kinetic energy limit $K_{\max} = 1$ J. We repeat the experiment for $\gamma \in \{1, 2, 10, 50\}$, as well as with the CBF disabled.

The end-effector trajectories (y-position) are shown in Fig. 3, with the corresponding kinetic energy in Fig. 4. The latter shows that the CBF layer effectively limits the kinetic energy, becoming more conservative with lower values of γ. In contrast, for the case without CBF, the kinetic energy reaches up to 2.3 J.

Fig. 5 shows the power input of the CBF for each of these experiments, given by $\dot{\boldsymbol{q}}^\top(\boldsymbol{u}_{\text{des}} - \boldsymbol{u})$. For all experiments, total CBF power can be observed to be non-positive, demonstrating that the safety filter only applies damping to the system. Notice that on a joint level the injected power may indeed be positive, however the total power input is always non-positive. Fig. 6 shows the associated joint control torques for the experiment where $\gamma = 50$. The commanded input $\boldsymbol{u}$ closely follows the desired input $\boldsymbol{u}_{\text{des}}$ and only intervenes when necessary, demonstrating that the safety filter is minimally invasive.

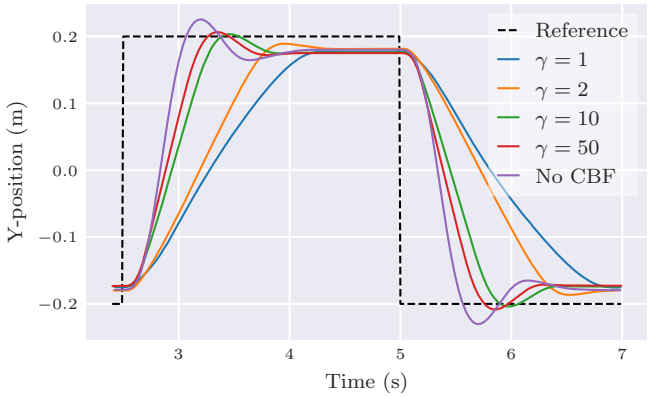

Fig. 3: Step response experiment: End-effector horizontal position.

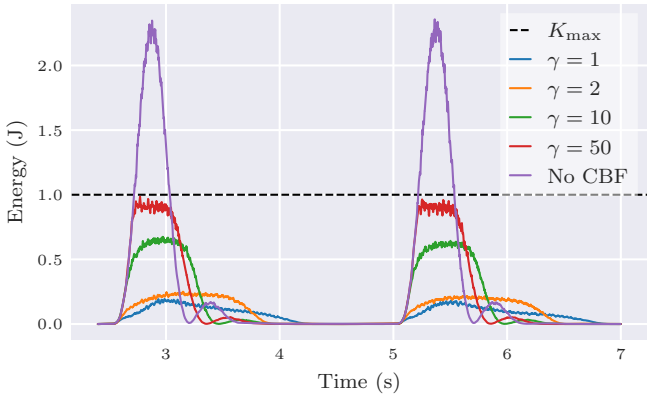

Fig. 4: Step response experiment: Total kinetic energy.

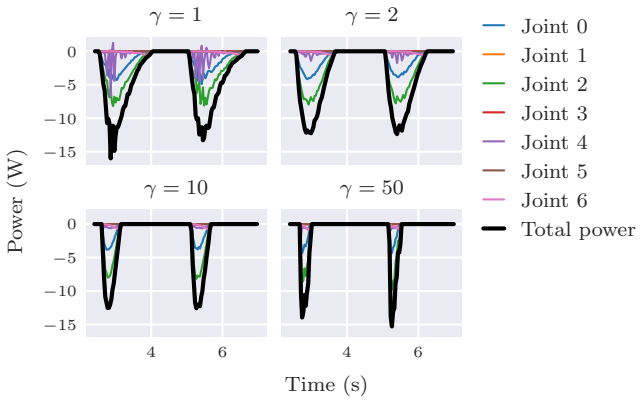

Fig. 5: Step response experiment: Safety filter power injection.

D. Contact loss

In this experiment, a string is attached to the end-effector and brought under 50 N of tension by lifting the equilibrium

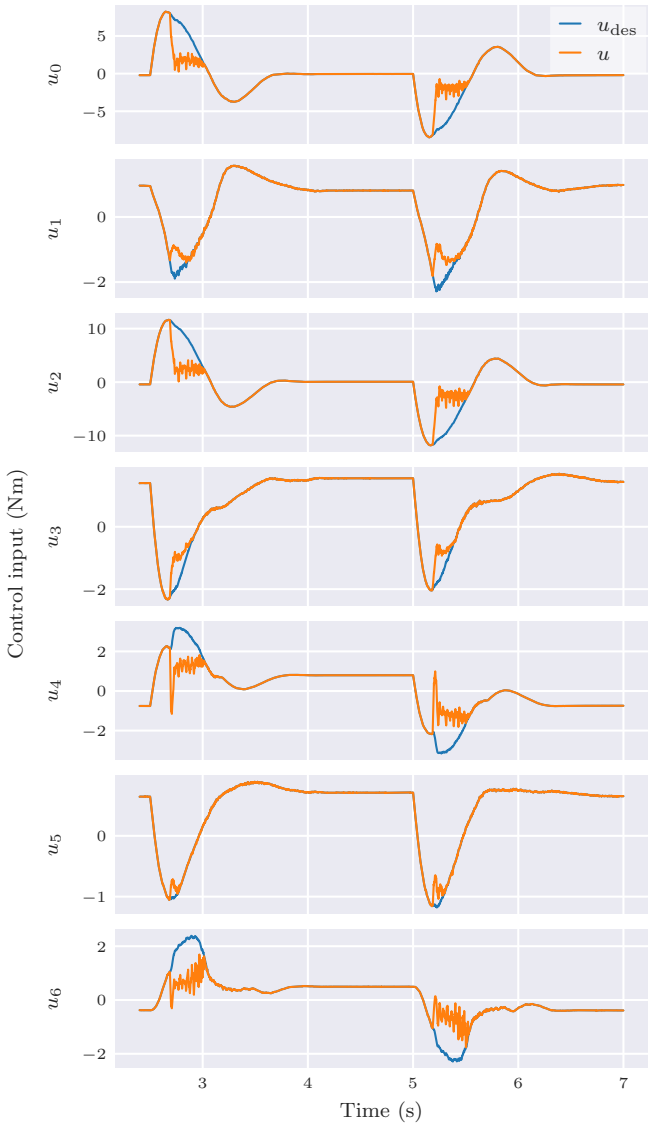

Fig. 6: Step response experiment: Nominal desired control action compared to the filtered control action ($\gamma = 50$).

setpoint of the Cartesian impedance controller, resulting in approximately 6 J of stored energy in the virtual spring. Upon release of the string, this energy is released and the end-effector rapidly moves up towards the equilibrium, as shown in Fig. 7. This is similar to the robot slipping off a surface it is pushing against in a sudden loss-of-contact scenario. The experiment is again repeated for $\gamma \in \{1, 2, 10, 50\}$ and without the CBF filter.

The total kinetic energy is shown in Fig. 8 and the CBF power injection in can be seen in Fig. 9. The former shows that approx. 1.7 J of kinetic energy is released by the nominal controller, and that this release is effectively compensated when the safety filter is activated. For $\gamma = 50$ the energy limit is momentarily exceeded, which we contribute to limited torque tracking capability of the robot actuators. However, this breach is small, and cases with more conservative values of γ remain far from the boundary. The plots in Fig. 9 show the total CBF power input, which is negative for all experiments. This confirms that the CBF only injected damping.

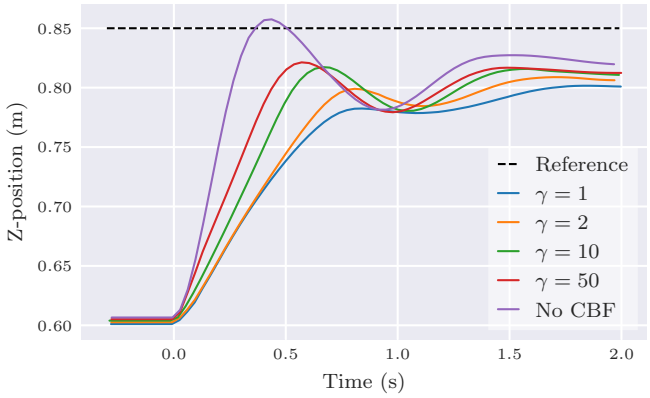

Fig. 7: Contact loss experiment: End-effector z-position.

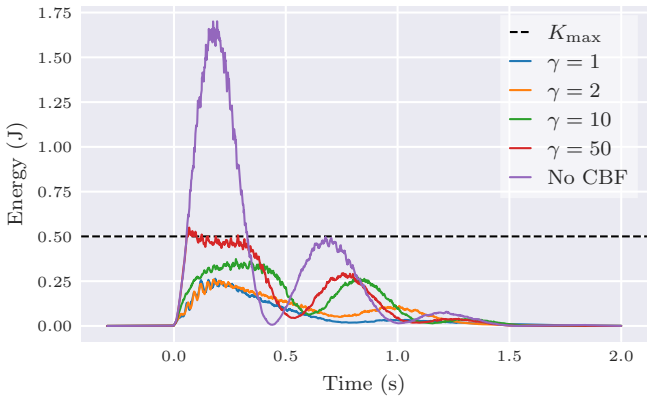

Fig. 8: Contact loss experiment: Total kinetic energy.

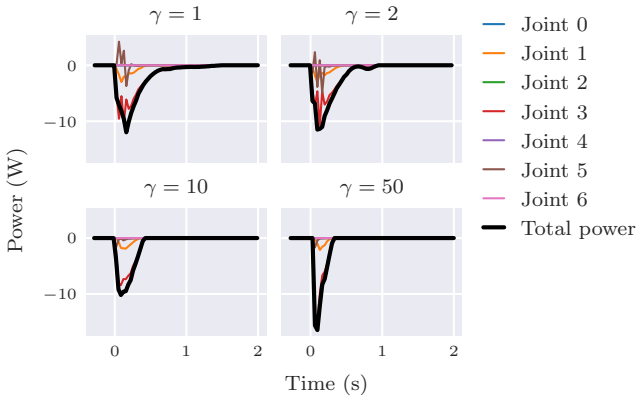

Fig. 9: Contact loss experiment: Safety filter power.

E. External interaction

In the final interaction experiments, we disable the nominal controller ($\boldsymbol{u}_{\text{des}} = \mathbf{0}$) and subject the robot to an unmodeled external power input.

In the first interaction experiment, we set $K_{\max} = 0\,\text{J}$ and inject external power by applying a virtual horizontal force to the end-effector. The force is regulated to provide a constant

power input. The kinetic energy is measured at steady-state, which occurs when the external input power and CBF damping are at equilibrium. This experiment is repeated for various power input values and $\gamma \in \{5, 10, 20, 30, 40, 50\}$.

Fig. 10 displays the steady-state kinetic energy (error) as function of the input power for different values of γ. One can see that unmodelled power inputs cause the robot to break the kinetic energy limit, and that the extent is lower for higher values of γ. Linear least-squares fitting (dashed lines) closely matches the the relation predicted by Eq. (20), as the slope of each curve is approx. γ^{-1}.

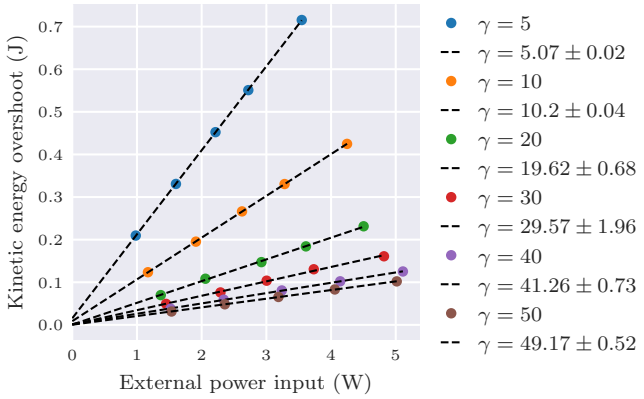

Fig. 10: Interaction experiment: Kinetic energy error versus external unmodelled power input, with fitted linear curves.

In the second interaction experiment, we physically push the end-effector for three different control cases: one without an active safety filter, one with the interaction-agnostic filter (Eq. (9)) and one which estimates and compensates for external torques (Eq. (23)). The kinetic energy limit is set to 0.3 J.

The kinetic energy after each push can be observed in Fig. 11. Three relevant power flows are shown in Fig. 12: The total power injected by the operator, the safety filter power injection, which is the only control power injection for this experiment, and the sum of both, which is the total power input into the system. Although the three experiments are not identical, the maximum power input is of similar magnitude. The red zones in this figure indicate when the robot is exceeding the energy limit.

We observe that both the interaction-agnostic and interaction-aware safety filters decrease the kinetic energy overshoot compared to the experiment without safety filter. The interaction-agnostic filter keeps the energy error below 0.5 J, which is the predicted limit given Eq. (20) and the 25 W peak external power input of Fig. 12. The damping in this experiment never exceeds the power input, as the combined power is always positive. The interaction-aware controller was expected to stay below the energy limit, but the limit is exceeded, which we attribute to imperfect estimation of the external interaction torques. However, the damping does exceed the input power when the kinetic energy limit is broken, demonstrating the additional damping the estimator provides.

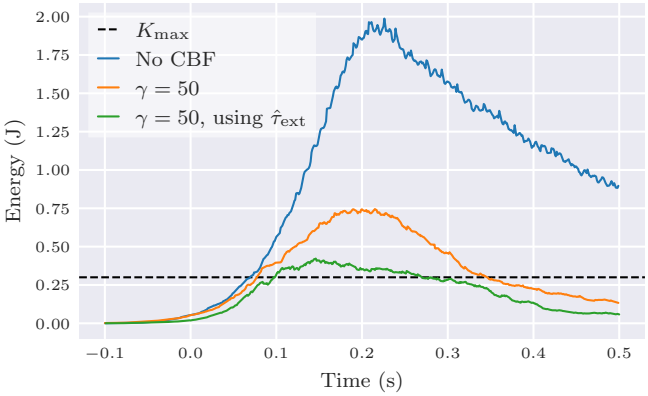

Fig. 11: Interaction experiment: Total kinetic energy.

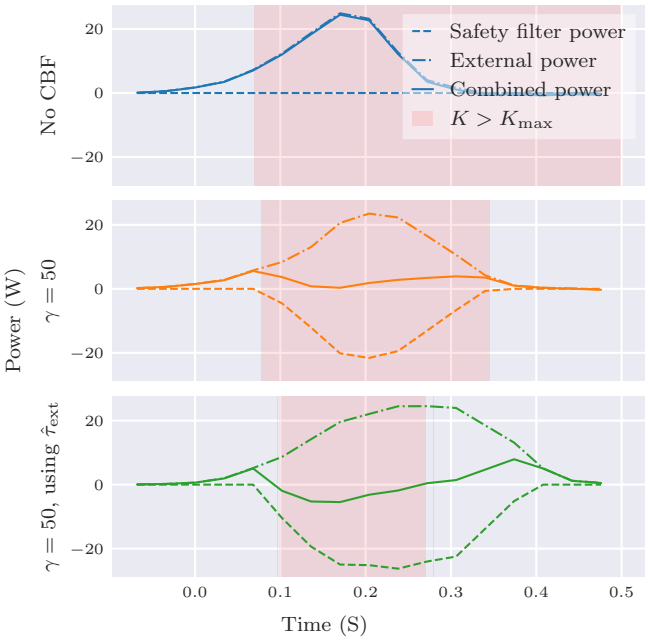

Fig. 12: Interaction experiment: Internal and external power injection for $\gamma = 50$. The red zone indicates where the robot exceeds its kinetic energy limit.

IV. Conclusions and Future Work

In this work we presented a new energy-based CBF control method that limits the kinetic energy of a robotic system and preserves passivity of the underlying nominal controller. The effect of unmodelled external forces was quantified and an extension to this method was made to counteract them.

The experimental results demonstrate that the presented control method effectively limits kinetic energy under a variety of scenarios by imposing a damping action on a nominal control task. Kinetic energy errors due to unmodelled power inputs are shown to be bounded by the safety layer, and can be reduced even further using external torque estimation. To the best of the author's knowledge, it is the first time that this form of control is verified experimentally on a torque-controlled robotic manipulator.

Future improvements include testing the algorithm on a system without built-in friction and gravity compensation.

For the experiments presented here, the control algorithm cannot account for potential errors in these control inputs, possibly reducing effectiveness. Another issue to be addressed is the system's sensitivity to noise. As previously stated, the control input scales with the third power of the joint velocity measurement, which for this setup is a discrete derivative of the joint position for this manipulator. Therefore, improved state estimation may be beneficial.

An extension to this research would be to not only limit the kinetic energy, but also the power and force transferred to the environment. This would cover all collision hazards as described by [6] and is also a requirement for safe, deliberate, long-term operator interaction. As discussed, accounting for external torques does not necessarily lead to safer interaction, as it could lead to more energy being transferred to the environment. Additionally, limiting the kinetic energy does not limit the total interaction force, which may still do harm in slow, forceful interactions. This extension may take the form of a secondary CBF that has to be satisfied concurrently. However, interaction power is not readily defined in the robot's state, which is how the CBF is defined. Therefore, such an extension is not trivial.

A second, more complex extension addresses the fact that kinetic energy is non-directional. Regardless of where the operator is, the robot will always limit its kinetic energy. Preferably, the robot would be allowed to move freely when moving away from the operator but limit its energy during approach. Because energy is scalar, this type of constraint lends itself more to a momentum-based CBF. The inherent necessity to define this problem in the task space makes derivation of the CBF function and, especially, its temporal derivative mathematically convoluted.

Acknowledgment

The author would first and foremost like to thank Federico and Wesley for their outstanding supervision of this thesis. Above all, their enthusiasm for the topic fueled mine and motivated me throughout the process.

Special thanks go out to Jan Broenink and Gwenn Englebienne for being part of the graduation committee. Stefano Stramigioli, who provided feedback during the green-light meeting, must also be acknowledged here.

I would like to extend my gratitude to the secretary and technicians at RAM. All research here, including mine, relies on their practical support and should not be undervalued.

My final thanks go out to my family, friends at RAM and fellow RSK'ers for showing interest during the process and sharing their insights.

References

[1] L. Brunke, M. Greeff, A. W. Hall, Z. Yuan, S. Zhou, J. Panerati, and A. P. Schoellig, "Safe Learning in Robotics: From Learning-Based Control to Safe Reinforcement Learning," *Annual Review of Control, Robotics, and Autonomous Systems*, vol. 5, no. 1, pp. 411–444, 5 2022.

[2] International Organization for Standardization, "Robots and robotic devices - Collaborative robots (ISO Standard No. 15066:2016)," 2 2016. [Online]. Available: https://www.iso.org/standard/62996.html

[3] T. Malm, T. Salmi, I. Marstio, and J. Montonen, "Dynamic safety system for collaboration of operators and industrial robots," *Open Engineering*, vol. 9, no. 1, pp. 61–71, 3 2019.

[4] Y. Kishi, Zhi Wei Luo, F. Asano, and S. Hosoe, "Passive impedance control with time-varying impedance center," in *Proceedings 2003 IEEE International Symposium on Computational Intelligence in Robotics and Automation. Computational Intelligence in Robotics and Automation for the New Millennium (Cat. No.03EX694)*. IEEE, 2003, pp. 1207–1212.

[5] D. Tsetserukou, R. Tadakuma, H. Kajimoto, N. Kawakami, and S. Tachi, "Towards Safe Human-Robot Interaction: Joint Impedance Control of a New Teleoperated Robot Arm," in *RO-MAN 2007 - The 16th IEEE International Symposium on Robot and Human Interactive Communication*. IEEE, 2007, pp. 860–865.

[6] S. Haddadin and E. Croft, "Physical Human–Robot Interaction," in *Springer Handbook of Robotics*, 2016, pp. 1839–1840.

[7] A. D. Ames, S. Coogan, M. Egerstedt, G. Notomista, K. Sreenath, and P. Tabuada, "Control barrier functions: Theory and applications," *2019 18th European Control Conference, ECC 2019*, pp. 3420–3431, 2019.

[8] W. S. Cortez and D. V. Dimarogonas, "Correct-by-Design Control Barrier Functions for Euler-Lagrange Systems with Input Constraints," in *2020 American Control Conference (ACC)*. IEEE, 7 2020, pp. 950–955.

[9] C. T. Landi, F. Ferraguti, S. Costi, M. Bonfe, and C. Secchi, "Safety barrier functions for human-robot interaction with industrial manipulators," in *2019 18th European Control Conference, ECC 2019*, 2019.

[10] M. Rauscher, M. Kimmel, and S. Hirche, "Constrained robot control using control barrier functions," in *2016 IEEE/RSJ International Conference on Intelligent Robots and Systems (IROS)*. IEEE, 10 2016, pp. 279–285.

[11] F. Ferraguti, C. T. Landi, A. Singletary, H.-C. Lin, A. Ames, C. Secchi, and M. Bonfè, "Safety and Efficiency in Robotics: The Control Barrier Functions Approach," 2022, pp. 15–30. [Online]. Available: https://ieeexplore.ieee.org/document/9788028

[12] A. Singletary, S. Kolathaya, and A. D. Ames, "Safety-Critical Kinematic Control of Robotic Systems," *Proceedings of the American Control Conference*, vol. 2021-May, pp. 14–19, 2021.

[13] Y. Michel, M. Saveriano, and D. Lee, "A Novel Safety-Aware Energy Tank Formulation Based on Control Barrier Functions," *IEEE Robotics and Automation Letters*, vol. 9, no. 6, pp. 5206–5213, 6 2024.

[14] F. Califano, "Passivity-Preserving Safety-Critical Control Using Control Barrier Functions," *IEEE Control Systems Letters*, vol. 7, pp. 1742–1747, 2023. [Online]. Available: https://ieeexplore.ieee.org/document/10136379/

[15] B. Stellato, G. Banjac, P. Goulart, A. Bemporad, and S. Boyd, "OSQP: an operator splitting solver for quadratic programs," *Mathematical Programming Computation*, vol. 12, no. 4, pp. 637–672, 12 2020.